Mean Field Games with Congestion Effects

Maxime EIDELSBERG
Simon SHEN

March 6, 2025

1 Introduction

This project focuses on the study of Mean Field Games (MFG) with congestion effects. MFGs were introduced by J-M. Lasry and P-L. Lions to analyze deterministic or stochastic differential games when the number of players tends to infinity. In this framework, players are assumed to be indistinguishable and have a negligible influence on the game. Each individual strategy is influenced by averages of quantities depending on the states or controls of the other players.

The objective of this project is to numerically simulate MFGs with congestion effects using finite difference schemes. We will also compare the results obtained with those of a Mean Field Control (MFC) problem.

2 Mathematical Model

2.1 Mathematical Formulation

Consider a state space $\mathbb{R}^d$ and a finite time horizon $T > 0$. For a typical player, the evolution of their state X_t^v is governed by the following stochastic differential equation (SDE):

$$dX_t^v = b(X_t^v, m(t, X_t^v), v(t, X_t^v))\, dt + \sigma\, dW_t, \quad t \geq 0, \tag{1}$$

where:

- $b : \mathbb{R}^d \times \mathbb{R} \times \mathbb{R}^d \to \mathbb{R}^d$ is the drift function,
- σ is the volatility,
- W_t is a standard Brownian motion,
- X_0^v is an independent random variable in $\mathbb{R}^d$, distributed according to the law m_0.

The total cost for a player using strategy v is given by :

$$J_m(v) = \mathbb{E}\left[\int_0^T f(X_t^v, m(t, X_t^v), v(t, X_t^v))\, dt + \phi(X_T^v, m(T, X_T^v))\right], \tag{2}$$

where:

- $f : \mathbb{R}^d \times \mathbb{R} \times \mathbb{R}^d \to \mathbb{R}$ is the running cost,
- $\phi : \mathbb{R}^d \times \mathbb{R} \to \mathbb{R}$ is the terminal cost.

2.2 Nash Equilibrium

A Nash equilibrium for this game is characterized by a pair $(\hat{m}, \hat{v})$ such that:

1. $\hat{v}$ minimizes the cost $J_{\hat{m}}(v)$ under the constraint that X_t^v follows the SDE (1).
2. For all $t \in [0,T]$, $\hat{m}(t,\cdot)$ is the law of $X_t^{\hat{v}}$.

The goal of this project is to find this equilibrium while incorporating congestion effects.

2.3 Hamilton-Jacobi-Bellman (HJB) and Kolmogorov-Fokker-Planck (KFP) Equations

Using the Hamilton-Jacobi-Bellman (HJB) and Kolmogorov-Fokker-Planck (KFP) equations, the Nash equilibrium can be characterized by a coupled system of partial differential equations (PDEs):

$$\begin{cases} -\dfrac{\partial u}{\partial t}(t,x) - \nu\Delta u(t,x) + H(x, m(t,x), \nabla u(t,x)) = 0, \quad \text{in } [0,T) \times \mathbb{R}^d, & (3) \\ \dfrac{\partial m}{\partial t}(t,x) - \nu\Delta m(t,x) - \operatorname{div}\left(m(t,\cdot) H_p(\cdot, m(t,\cdot), \nabla u(t,\cdot))\right) = 0, \quad \text{in } (0,T] \times \mathbb{R}^d, & (4) \end{cases}$$

with terminal/initial conditions:

$$u(T,x) = \phi(x, m(T,x)), \quad m(0,x) = m_0(x), \quad \text{in } \mathbb{R}^d. \tag{5}$$

Here, H is the Hamiltonian defined by:

$$H(x,m,p) = \max_{\gamma \in \mathbb{R}^d} \left\{ -f(x,m,\gamma) - \langle b(x,m,\gamma), p \rangle \right\}. \tag{6}$$

Thus, the Nash equilibrium control $\hat{v}$ is given by:

$$\hat{v}(t,x) = \arg\max_{a \in \mathbb{R}^d} \left\{ -f(x, m(t,x), a) - \langle b(x, m(t,x), a), \nabla u(t,x) \rangle \right\}$$

2.4 Fundamental Equations for the Congestion Model

We consider a congestion model where $b(x,m,\gamma) = \gamma$, and the running cost takes the form:

$$f(x,m,\gamma) = L_0(\gamma, m(x)) + f_0(x, m(x)),$$

where $L_0 : \mathbb{R}^d \times \mathbb{R}_+ \to \mathbb{R}$ is given by :

$$L_0(\gamma, \mu) = \frac{\beta - 1}{\beta} \left(c_0 + c_1 \mu\right)^{\frac{\alpha}{\beta - 1}} |\gamma|^{\frac{\beta}{\beta - 1}}.$$

The parameters satisfy the following conditions:

- $\beta > 1$,
- $0 \leq \alpha \leq \frac{4(\beta-1)}{\beta}$,
- $c_0 \geq 0$,

- $c_1 > 0$.

The associated Hamiltonian is then:

$$H(x, m, p) = \max_{\gamma \in \mathbb{R}^d} \{-L_0(\gamma, m(x)) - \langle \gamma, p \rangle\} - f_0(x, m(x)).$$

Using the expression for L_0, we obtain:

$$H(x, m, p) = \frac{1}{\beta} \frac{|p|^\beta}{(c_0 + c_1 m(x))^\alpha} - f_0(x, m(x)).$$

Furthermore, we assume that the running cost f_0 decomposes as:

$$f_0(x, m(x)) = \tilde{f}_0(m(x)) + g(x),$$

where :

- $\tilde{f}_0 : \mathbb{R}_+ \to \mathbb{R}$ is a smooth function,
- $g : \mathbb{R}^d \to \mathbb{R}$ is a given function.

This decomposition simplifies the discrete Hamiltonian and facilitates the numerical implementation of the finite difference scheme.

A natural choice for the discrete Hamiltonian is:

$$\hat{H}(p_1, p_2, \mu) = \frac{1}{\beta} \frac{\left((p_1)_+^2 + (p_2)_-^2\right)^{\beta/2}}{(c_0 + c_1 \mu)^\alpha},$$

where $(p_1)_+$ and $(p_2)_-$ denote the positive and negative parts of p_1 and p_2, respectively.

This discrete Hamiltonian satisfies the following properties:

- **Monotonicity**: Ensures uniqueness of the solution for the discrete HJB and KFP equations and guarantees that the solution of the discrete KFP equation remains non-negative if the initial condition is non-negative.
- **Consistency**: Essential for the numerical scheme to converge to the continuous solution as the discretization step tends to zero.
- **Differentiability**: Allows the use of Newton's method to efficiently solve the discrete HJB equation.

2.5 Forward-Backward System for Congestion MFG

For an MFG with congestion effects, the forward-backward system is given by:

$$\begin{cases} -\dfrac{\partial u}{\partial t}(t,x) - \nu \Delta u(t,x) + \dfrac{1}{\beta} \dfrac{|\nabla u(t,x)|^\beta}{(c_0 + c_1 m(t,x))^\alpha} = f_0(x, m(t,x)) & (7) \\ \dfrac{\partial m}{\partial t}(t,x) - \nu \Delta m(t,x) - \operatorname{div}\left(\dfrac{m(t,\cdot)}{(c_0 + c_1 m(t,\cdot))^\alpha} |\nabla u(t,\cdot)|^{\beta-2} \nabla u(t,\cdot) \right) = 0 & (8) \end{cases}$$

with Neumann boundary conditions:

$$\frac{\partial u}{\partial x}(t,0) = \frac{\partial u}{\partial x}(t,1) = 0 \tag{9}$$

$$\frac{\partial m}{\partial x}(t,0) = \frac{\partial m}{\partial x}(t,1) = 0 \tag{10}$$

and terminal/initial conditions:

$$u(T,x) = \phi(x, m(T,x)), \quad m(0,x) = m_0(x) \tag{11}$$

3 Finite Difference Scheme

We use a finite difference scheme to discretize the HJB and KFP equations. Let N_T and N_h be two positive integers. We consider N_T+1 time points and N_h spatial points, respectively. Define $\Delta t = T/N_T$, $h = 1/(N_h-1)$, and $t_n = n \cdot \Delta t$, $x_i = i \cdot h$ for $(n,i) \in \{0,\dots,N_T\} \times \{0,\dots,N_h-1\}$. We approximate u and m with the vectors U and M in $\mathbb{R}^{(N_T+1)\times N_h}$, such that $u(t_n,x_i) \approx U_i^n$ and $m(t_n,x_i) \approx M_i^n$ for each (n,i) in $\{0,\dots,N_T\} \times \{0,\dots,N_h-1\}$.

To account for Neumann boundary conditions, we introduce ghost nodes $x_{-1} = -h$, $x_{N_h} = 1+h$ and set:

$$U_{-1}^n = U_0^n, \quad U_{N_h}^n = U_{N_h-1}^n, \quad M_{-1}^n = M_0^n, \quad M_{N_h}^n = M_{N_h-1}^n$$

3.1 Finite Difference Operators

We define the following operators:

$$\partial_t w(t_n,x) \longleftrightarrow (D_t W)^n = \frac{W^{n+1}-W^n}{\Delta t}, \quad n \in \{0,\dots,N_T-1\}, \quad W \in \mathbb{R}^{N_T+1}$$

$$\partial_x w(t,x) \longleftrightarrow (DW)_i = \frac{W_{i+1}-W_i}{h}, \quad i \in \{0,\dots,N_h-1\}, \quad W \in \mathbb{R}^{N_h}$$

$$\partial_x^2 w(t,x_i) \longleftrightarrow (\Delta_h W)_i = \frac{W_{i+1}-2W_i+W_{i-1}}{h^2}, \quad i \in \{0,\dots,N_h-1\}, \quad W \in \mathbb{R}^{N_h}$$

$$[\nabla_h W]_i = ((DW)_i, (DW)_{i-1}), \quad i \in \{0,\dots,N_h-1\}, \quad W \in \mathbb{R}^{N_h}$$

These can be expressed in matrix form. For a matrix $W \in \mathbb{R}^{(N_T+1)\times N_h}$, we have:

$$(\partial_x(t_n,x_i))_{\substack{0\le n\le N_T \\ 0\le i\le N_h-1}} \longleftrightarrow \frac{1}{h}\begin{pmatrix} -1 & 1 & 0 & 0 & \cdots & 0 \\ 0 & -1 & 1 & 0 & \cdots & 0 \\ 0 & 0 & -1 & 1 & \cdots & 0 \\ \vdots & & \ddots & \ddots & \vdots & \\ 0 & 0 & \cdots & 0 & -1 & 1 \\ 0 & 0 & \cdots & 0 & 0 & 0 \end{pmatrix} \begin{pmatrix} W_0^0 & W_0^1 & \cdots & W_0^{N_T} \\ W_1^1 & W_1^1 & \cdots & W_1^{N_T} \\ \vdots & \vdots & \ddots & \vdots \\ W_{N_h-1}^0 & W_{N_h-1}^1 & \cdots & W_{N_h-1}^{N_T} \end{pmatrix}$$

The last column accounts for Neumann conditions, where $U_{N_h} = U_{N_h-1}$ and $M_{N_h} = M_{N_h-1}$. Let D_x denote this matrix.

Similarly, the second derivative is approximated by:

$$\left(\partial_x^2(t_n, x_i)\right)_{\substack{0\le n\le N_T \\ 0\le i\le N_h-1}} \longleftrightarrow \frac{1}{h^2}\begin{pmatrix} -1 & 1 & 0 & 0 & \cdots & 0 \\ 1 & -2 & 1 & 0 & \cdots & 0 \\ 0 & 1 & -2 & 1 & \cdots & 0 \\ \vdots & & \ddots & \ddots & \vdots & \\ 0 & 0 & \cdots & 0 & -2 & 1 \\ 0 & 0 & \cdots & 0 & 1 & -1 \end{pmatrix}\begin{pmatrix} W_0^0 & W_0^1 & \cdots & W_0^{N_T} \\ W_1^1 & W_1^1 & \cdots & W_1^{N_T} \\ \vdots & \vdots & \ddots & \vdots \\ W_{N_h-1}^0 & W_{N_h-1}^1 & \cdots & W_{N_h-1}^{N_T} \end{pmatrix}$$

Let D_x^2 denote this matrix.

The backward difference operator ($(DW)_{i-1} = \frac{1}{h}(W_i - W_{i-1}))_{0\le i<N_h}$ is given by (because of Neumann's Conditions):

$$\frac{1}{h}\begin{pmatrix} 0 & 0 & 0 & 0 & \cdots & 0 \\ -1 & 1 & 0 & 0 & \cdots & 0 \\ 0 & -1 & 1 & 0 & \cdots & 0 \\ \vdots & & \ddots & \ddots & \vdots & \\ 0 & 0 & \cdots & 0 & 1 & 0 \\ 0 & 0 & \cdots & 0 & -1 & 1 \end{pmatrix}$$

3.2 Solving the HJB Equation

The discretized HJB equation is solved using a Newton-Raphson method.

The discretized HJB equation, by using the discrete Hamiltonian previously defined, is given by:

$$\begin{cases} -(D_tU_i)^n - \nu(\Delta_h U^n)_i + \tilde{H}(x_i, [\nabla_h U^n]_i) = g(x_i) + \tilde{f}_0(M_i^{n+1}), & 0 \le i < N_h, 0 \le n < N_T \\ U_{-1}^n = U_0^n, & 0 \le n < N_T \\ U_{N_h}^n = U_{N_h-1}^n, & 0 \le n < N_T \\ U_i^{N_T} = \phi(x_i, M_i^{N_T}), & 0 \le i < N_h \end{cases}$$

This is an implicit Euler scheme since the equation is backward in time. To compute M^{n+1} and U^{n+1}, we define

$$\mathcal{F}(U^n, U^{n+1}, M^{n+1}) := \begin{pmatrix} -(D_tU_0)^n - \nu(\Delta_h U^n)_0 + \tilde{H}(x_0, [\nabla_h U^n]_0) - g(x_i) - \tilde{f}_0(M_i^{n+1}) \\ \vdots \\ -(D_tU_i)^n - \nu(\Delta_h U^n)_i + \tilde{H}(x_i, [\nabla_h U^n]_i) - g(x_i) - \tilde{f}_0(M_i^{n+1}) \\ \vdots \\ -(D_tU_{N_h-1})^n - \nu(\Delta_h U^n)_{N_h-1} + \tilde{H}(x_{N_h-1}, [\nabla_h U^n]_{N_h-1}) - g(x_i) - \tilde{f}_0(M_i^{n+1}) \end{pmatrix}$$

When solving the HJB equation, the goal is to find U^n given U^{n+1} and M^{n+1}. The terminal condition $U_i^{N_T} = \phi(M_i^{N_T})$ initializes the solution at $n = N_T$. For $n < N_T$, we use Newton-Raphson, estimating U^n as the limit of the sequence $(U^{n,k})_k$ defined by:

$$U^{n,k+1} = U^{n,k} - \mathcal{J}^{-1}(U^{n,k}, U^{n+1}, M^{n+1})\mathcal{F}(U^{n,k}, U^{n+1}, M^{n+1})$$

where $\mathcal{J}^{-1}(V, U^{n+1}, M^{n+1})$ is the Jacobian of the map $V \mapsto \mathcal{F}(V, U^{n+1}, M^{n+1})$. We initialize $U^{n,0} = U^{n+1}$. Newton iterations stop when $\|\mathcal{F}(U^{n,k}, U^{n+1}, M^{n+1})\|$ falls below a threshold of 10^{-12}.

3.3 Closed-Form Jacobian

Let $\mathcal{F}_i$ denote the i-th component of $\mathcal{F}(U^n, U^{n+1}, M^{n+1})$. The Jacobian matrix is:

$$\mathcal{J}(V, U^{n+1}, M^{n+1}) = \begin{pmatrix} \frac{\partial \mathcal{F}_0}{\partial V_0} & \frac{\partial \mathcal{F}_0}{\partial V_1} & \cdots & \frac{\partial \mathcal{F}_0}{\partial V_{N_h-1}} \\ \frac{\partial \mathcal{F}_1}{\partial V_0} & \frac{\partial \mathcal{F}_1}{\partial V_1} & \cdots & \frac{\partial \mathcal{F}_1}{\partial V_{N_h-1}} \\ \vdots & \vdots & \ddots & \vdots \\ \frac{\partial \mathcal{F}_{N_h-1}}{\partial V_0} & \frac{\partial \mathcal{F}_{N_h-1}}{\partial V_1} & \cdots & \frac{\partial \mathcal{F}_{N_h-1}}{\partial V_{N_h-1}} \end{pmatrix}$$

Observe that (letting $A = -g(x_i) - \tilde{f}_0(M_i^{n+1})$):

$$\mathcal{F}_i = -(D_t U_i)^n - \nu(\Delta_h U^n)_i + \tilde{H}(x_i, [\nabla_h U^n]_i) - g(x_i) - \tilde{f}_0(M_i^{n+1})$$

$$= -\frac{U_i^{n+1} - U_i^n}{\Delta t} - \nu\frac{U_{i+1}^n - 2U_i^n + U_{i-1}^n}{h^2} + \frac{1}{\beta h^\beta (c_0 + c_1 M_i)^\alpha}\left((U_{i+1}^n - U_i^n)^2 + (U_i^n - U_{i-1}^n)^2\right)^{\beta/2} + A$$

This term depends only on $U_{i-1}^n, U_i^n, U_{i+1}^n$, so the Jacobian is tri-diagonal. We obtain:

$$\frac{\partial \mathcal{F}_i}{\partial U_{i-1}^n} = -\frac{\nu}{h^2} - \frac{1}{h^\beta (c_0 + c_1 M_i)^\alpha}(U_i^n - U_{i-1}^n)_+ \left((U_{i+1}^n - U_i^n)^2 + (U_i^n - U_{i-1}^n)^2\right)^{\beta/2-1}$$

$$\frac{\partial \mathcal{F}_i}{\partial U_i^n} = \frac{1}{\Delta t} + \frac{2\nu}{h^2} + \frac{1}{h^\beta (c_0 + c_1 M_i)^\alpha}\left((U_{i+1}^n - U_i^n)_- + (U_i^n - U_{i-1}^n)_+\right)\left((U_{i+1}^n - U_i^n)^2 + (U_i^n - U_{i-1}^n)^2\right)^{\beta/2-1}$$

$$\frac{\partial \mathcal{F}_i}{\partial U_{i+1}^n} = -\frac{\nu}{h^2} - \frac{1}{h^\beta (c_0 + c_1 M_i)^\alpha}(U_{i+1}^n - U_i^n)_- \left((U_{i+1}^n - U_i^n)^2 + (U_i^n - U_{i-1}^n)^2\right)^{\beta/2-1}$$

Let J_H denote the Jacobian of $U^n \mapsto (\tilde{H}(x_i, [\nabla_h U^n]_i))_{0 \le i < N_h}$ evaluated at U^n. This will be useful later. The resulting matrix is tri-diagonal such that:

$$(J_H)_{i,i-1} = -\frac{1}{h^\beta (c_0 + c_1 M_i)^\alpha}(U_i^n - U_{i-1}^n)_+ \left((U_{i+1}^n - U_i^n)^2 + (U_i^n - U_{i-1}^n)^2\right)^{\beta/2-1}$$

$$(J_H)_{i,i} = \frac{1}{h^\beta (c_0 + c_1 M_i)^\alpha}\left((U_{i+1}^n - U_i^n)_- + (U_i^n - U_{i-1}^n)_+\right)\left((U_{i+1}^n - U_i^n)^2 + (U_i^n - U_{i-1}^n)^2\right)^{\beta/2-1}$$

$$(J_H)_{i,i+1} = -\frac{1}{h^\beta (c_0 + c_1 M_i)^\alpha}(U_{i+1}^n - U_i^n)_- \left((U_{i+1}^n - U_i^n)^2 + (U_i^n - U_{i-1}^n)^2\right)^{\beta/2-1}$$

3.4 Solving the KFP Equation

To define an appropriate discretization of the KFP equation, we first discuss how to discretize $\partial_x \left(m(t,\cdot)|\partial_x u(t,\cdot)|^{\beta-2}\partial_x u(t,\cdot)\right)$. Recall that:

$$\partial_x \left(m(t,\cdot)|\partial_x u(t,\cdot)|^{\beta-2}\partial_x u(t,\cdot)\right)(x) = \partial_x \left(m(t,x)\partial_p H_0(x,\partial_x u(t,x))\right)$$

Consider a smooth function $w \in \mathcal{C}^\infty([0,T]\times\Omega)$. Using integration by parts and accounting for Neumann boundary conditions, and assuming $\partial_p H(x,0)=0$, we obtain:

$$-\int_\Omega \partial_x \left(m(t,x)\partial_p H_0(x,\partial_x u(t,x))\right) w(t,x)\,dx = \int_\Omega m(t,x)\partial_p H_0(x,\partial_x u(t,x))\partial_x w(t,x)\,dx$$

A natural approximation of the right-hand side is:

$$h\sum_{i=0}^{N_h-1} M_i^{n+1}\left(\partial_{p_1}\tilde{H}(x_i,[\nabla_h U^n]_i)\frac{W_{i+1}^n - W_i^n}{h} + \partial_{p_2}\tilde{H}(x_i,[\nabla_h U^n]_i)\frac{W_i^n - W_{i-1}^n}{h}\right)$$

By performing discrete integration by parts, we obtain the discrete equivalent of the left-hand side as $-h\sum_{i=0}^{N_h-1}\mathcal{T}_i(U^n,M^{n+1})W_i^n$, where:

$$\mathcal{T}_i(U,M) = \frac{1}{h}\left(M_i\partial_{p_1}\tilde{H}(x_i,[\nabla_h U^n]_i) - M_{i-1}\partial_{p_1}\tilde{H}(x_{i-1},[\nabla_h U^n]_{i-1})\right)$$

$$+\frac{1}{h}\left(M_{i+1}\partial_{p_2}\tilde{H}(x_{i+1},[\nabla_h U^n]_{i+1}) - M_i\partial_{p_2}\tilde{H}(x_i,[\nabla_h U^n]_i)\right)$$

We now consider the following discrete version of the KFP equation, supplemented with Neumann boundary conditions and the terminal condition:

$$\begin{cases} (D_t M_i)^n - \nu(\Delta_h M^{n+1})_i - \mathcal{T}_i(U^n,M^{n+1}) = 0, & 0\le i<N_h,\ 0\le n<N_T \\ M_{-1}^n = M_0^n, & 0<n\le N_T \\ M_{N_h}^n = M_{N_h-1}^n, & 0<n\le N_T \\ M_i^0 = \bar{m}_0(x_i), & 0\le i<N_h \end{cases}$$

where, for example:

$$\bar{m}_0(x_i) = \int_{|x-x_i|\le h/2} m_0(x)\,dx \quad \text{or} \quad \bar{m}_0(x_i) = m_0(x_i)$$

This scheme is implicit but, unlike the HJB scheme, it involves a forward loop. Starting from time step 0, $M_i^0 = \bar{m}_0(x_i)$ provides an explicit formula for M^0. The n-th step computes M^{n+1} given U^n and M^n. Since the KFP system is linear, it can be solved using basic linear algebra methods.

We introduce $\mathcal{T}(U,M) := (\mathcal{T}_0(U,M),\dots,\mathcal{T}_{N_h-1}(U,M))^T$. Note that $M \mapsto \mathcal{T}(U^n,M)$ is a linear operator. Let A be the associated matrix. Then $A = (-J_H)^T$.

Given that $(D_t M)^n = \frac{1}{\Delta t}(M^{n+1}-M^n)$, we can rewrite the system as:

$$\frac{M^{n+1}-M^n}{\Delta t} - \nu D_x^2 M^{n+1} + (J_H)^T M^{n+1} = 0$$

Finding M^{n+1} thus reduces to solving:

$$\left(I_{N_h} - \nu \Delta t D_x^2 + \Delta t (J_H)^T\right) M^{n+1} = M^n$$

This linear system can be efficiently solved using standard linear algebra techniques, ensuring that the solutionM^{n+1} is unique and consistent with the given boundary conditions.

3.5 Solving the Forward-Backward System

The main idea is to use Picard-type fixed-point iterations to compute $\mathcal{M} := (M^n)_{0 \le n \le N_T}$ and $\mathcal{U} := (U^n)_{0 \le n \le N_T}$.

Let $0 < \theta < 1$ be a parameter (e.g., $\theta = 0.01$). Let $(\mathcal{M}^{(k)}, \mathcal{U}^{(k)})$ be the current approximation of $(\mathcal{M}, \mathcal{U})$. The next approximation $(\mathcal{M}^{(k+1)}, \mathcal{U}^{(k+1)})$ is computed as follows:

- Solve the discrete HJB equation using $(\mathcal{M}^{(k)}, \mathcal{U}^{(k)})$. The solution is denoted $\hat{\mathcal{U}}^{(k+1)}$.
- Solve the discrete KFP equation using $(\mathcal{M}^{(k)}, \hat{\mathcal{U}}^{(k+1)})$. The solution is denoted $\hat{\mathcal{M}}^{(k+1)}$.
- Define $(\mathcal{M}^{(k+1)}, \mathcal{U}^{(k+1)}) = (1-\theta)(\mathcal{M}^{(k)}, \mathcal{U}^{(k)}) + \theta(\hat{\mathcal{M}}^{(k+1)}, \hat{\mathcal{U}}^{(k+1)})$.

The iterations stop when the norm of the increment $(\mathcal{M}^{(k+1)}, \mathcal{U}^{(k+1)}) - (\mathcal{M}^{(k)}, \mathcal{U}^{(k)})$ falls below a given threshold, e.g., 10^{-6}.

To initialize the loop, we set $M_i^{n,(0)} = \bar{m}_0(x_i)$ for all $0 \le i < N_h$ and $0 \le n \le N_T$. The initial value of $U^{(0)}$ has little impact on the algorithm's convergence. We set $U_i^{n,(0)} = 0$ for all i, n.

3.6 Implementation Remarks

- The Jacobian matrix $\mathcal{J}$ or HJB is sparse and can be assembled via finite differences.
- The operator $\mathcal{T}(U^n)$ in KFP is antisymmetric, ensuring mass conservation: $\sum_i M_i^n = \text{const}$.
- The parameter θ should be small (e.g., $0.01 \le \theta \le 0.2$)to ensure convergence. The parameter θ controls convergence speed : a smaller θ leads to slower but more stable convergence, while a larger θ may accelerate convergence at the risk of instability.

4 Initial Results

4.1 Parameters for Testing

Simulations of the Mean Field Game (MFG) are performed with the following parameters:

- Spatial domain: $\Omega =]0, 1[$
- Time horizon: $T = 1$
- Function $g(x)$: $g(x) = 0$

- Hamiltonian H_0: Given by:

$$H_0(p,\mu) = \frac{1}{\beta}\frac{|p|^\beta}{(c_0 + c_1\mu)^\alpha},$$

with the discrete Hamiltonian:

$$\hat{H}(p_1,p_2,\mu) = \frac{1}{\beta}\frac{\left((p_1)_+^2 + (p_2)_-^2\right)^{\beta/2}}{(c_0 + c_1\mu)^\alpha}.$$

- Parameter sets:
  1. $\beta = 2$, $c_0 = 0.1$, $c_1 = 1$, $\alpha = 0.5$, $\sigma = 0.02$
  2. $\beta = 2$, $c_0 = 0.1$, $c_1 = 5$, $\alpha = 1$, $\sigma = 0.02$
  3. $\beta = 2$, $c_0 = 0.01$, $c_1 = 2$, $\alpha = 1.2$, $\sigma = 0.1$
  4. $\beta = 2$, $c_0 = 0.01$, $c_1 = 2$, $\alpha = 1.5$, $\sigma = 0.2$
  5. $\beta = 2$, $c_0 = 1$, $c_1 = 3$, $\alpha = 2$, $\sigma = 0.002$
- Function $\tilde{f}_0$: $\tilde{f}_0(m(x)) = \frac{m(x)}{10}$
- Terminal cost ϕ: $\phi(x,m) = -\exp\left(-40(x-0.7)^2\right)$
- Initial condition m_0: $m_0(x) = \sqrt{\frac{300}{\pi}}\exp\left(-300(x-0.2)^2\right)$
- Discretization:
  - Spatial points: $N_h = 201$
  - Time points: $N_T = 100$
- Relaxation parameter θ: Chosen in $[0.001, 0.2]$ to ensure convergence. If the method does not converge, reduce θ.
- Stopping criteria:
  - Newton method: 10^{-12}
  - Fixed-point method: 2×10^{-5} (with normalized norms such that $\|(1,\ldots,1)\| = 1$)

4.2 Analysis of Results

We begin by plotting the contours of the HJB and Fokker-Planck solutions in the (x,t) plane.

4.2.1 Contours of the HJB Solution

For the contours of U, we generally observe that near $t \approx 1$ (top of the graph), the contours are tightly packed, indicating a strong gradient of $U(x,t)$ - i.e., large changes in value for small variations in x.

For smaller t, the contours become more spaced out, and the optimal value varies more smoothly with x. The purple color indicates lower U values, which is expected as time approaches 0 (no further optimization opportunities). This suggests convergence to a steady state.

Interpretation: Early in the time horizon (large t due to the backward system), decisions have a strong impact on U, while later, control opportunities diminish.

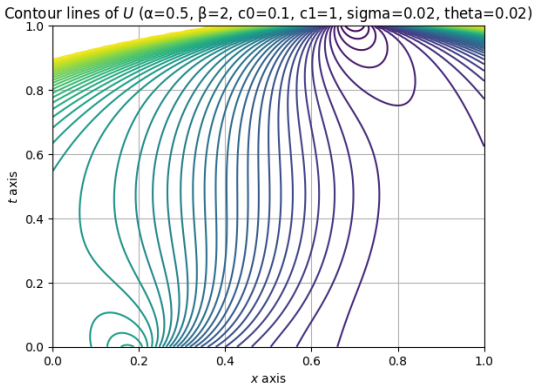

Figure 1: Contours of U (HJB solution)

4.2.2 Contours of the Fokker-Planck Solution

For the contours of M, two "nodes" appear at $t = 1$ and $t = 0$ at different positions. The node at $t = 0$ corresponds to the initial condition, and we observe a probability transition toward the node at $t = 1$, which can be interpreted as an optimal policy pushing the distribution in this direction.

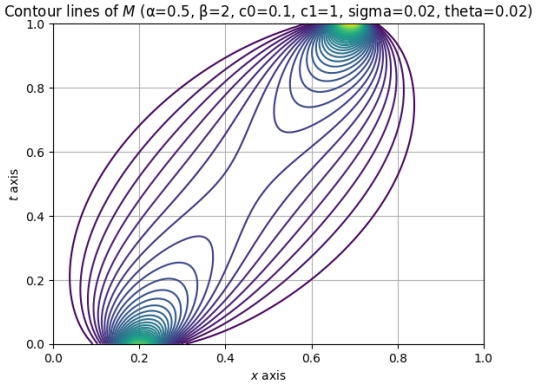

Figure 2: Contours of M(Fokker-Planck solution)

Results for the 5 Parameter Sets

4.3 Set 1: $\beta = 2$, $c_0 = 0.1$, $c_1 = 1$, $\alpha = 0.5$, $\sigma = 0.02$

4.3.1 Contours of U (HJB)

The contours of U show strong variation near $t = 1$, indicating a steep gradient of U at this time horizon. This suggests that decisions made early in the period have significant impact on the value of U. As t decreases, the contours become more spaced out, indicating smoother variation of U with x. This can be interpreted as convergence toward a steady state where control opportunities diminish.

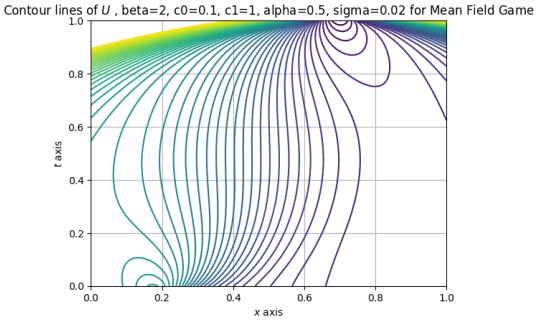

(a) Contours of U (parameters set 1)

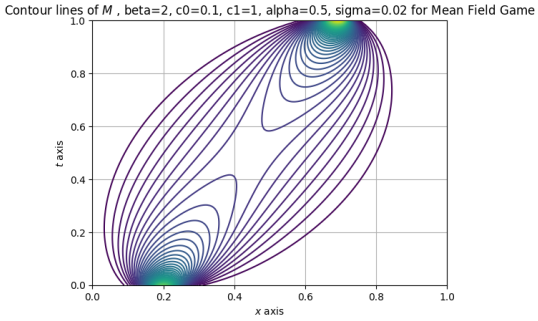

(b) Contours of M (parameters set 1)

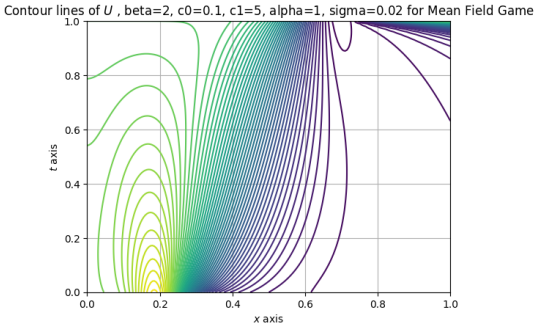

(c) Contours of U (parameters set 2)

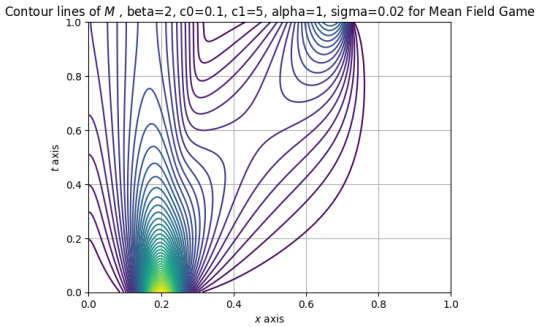

(d) Contours of M (parameters set 2)

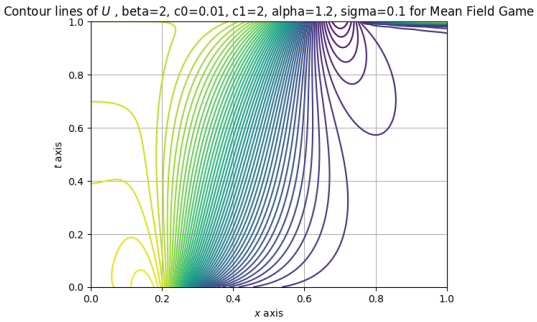

(e) Contours of U (parameters set 3)

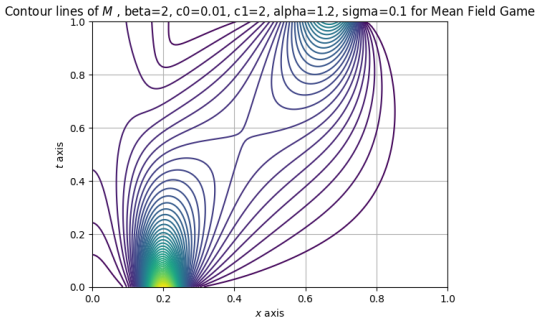

(f) Contours of M (parameters set 3)

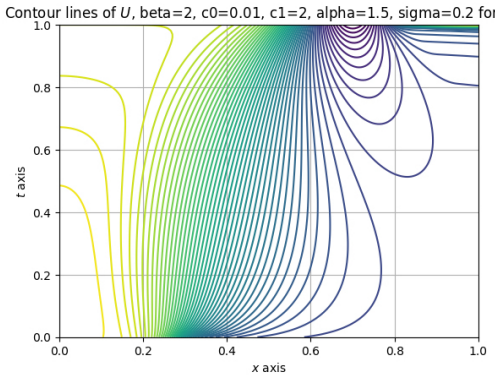

(a) Contours of U (parameters set 4)

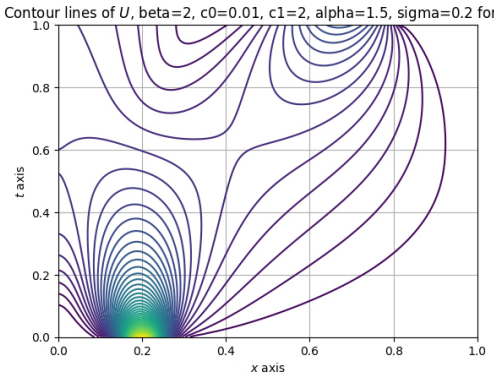

(b) Contours of M (parameters set 4)

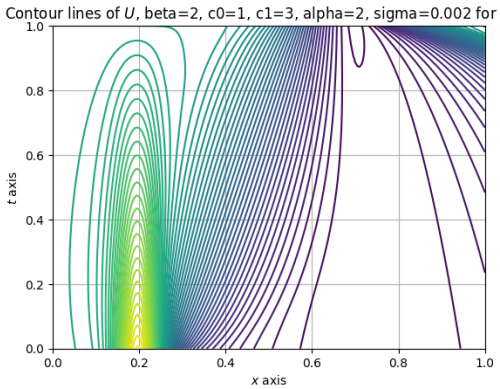

(c) Contours of U (parameters set 5)

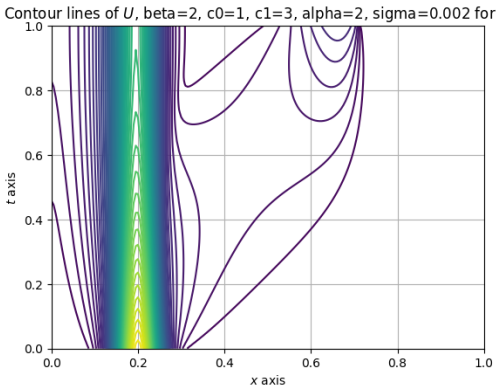

(d) Contours of M (parameters set 5)

Figure 4: Results: Contours of U and M

4.3.2 Contours of M (Fokker-Planck)

The contours of M show a clear transition between two "nodes" at horizons $t = 0$ and $t = 1$. This indicates an optimal policy that pushes the probability distribution toward a specific position at $t = 1$. The initial distribution at $t = 0$ is concentrated, then gradually diffuses toward the final position.

4.4 Set 2 : $\beta = 2$, $c_0 = 0.1$, $c_1 = 5$, $\alpha = 1$, $\sigma = 0.02$

4.4.1 Contours of U (HJB)

The contours of U show a structure similar to Set 1, but with more pronounced variations. This may be due to stronger congestion (higher c_1 value). The gradients are sharper, indicating greater sensitivity to decisions made early in the period.

4.4.2 Contours of M (Fokker-Planck)

The contours of M show faster diffusion and a less distinct transition between the two nodes. This may be due to stronger congestion ($\alpha = 1$). The initial distribution diffuses more rapidly, making the transition less marked.

4.5 Set 3 : $\beta = 2$, $c_0 = 0.01$, $c_1 = 2$, $\alpha = 1.2$, $\sigma = 0.1$

4.5.1 Contours of U (HJB)

The contours of U show broader diffusion, with less pronounced gradients than in previous cases. This may be due to even stronger congestion ($\alpha = 1.2$) and higher volatility ($\sigma = 0.1$). Decisions made early in the period have less localized impact, resulting in more gradual information diffusion.

4.5.2 Contours of M (Fokker-Planck)

The contours of M show very broad diffusion, with a very gradual transition between the two nodes. This is consistent with very strong congestion ($\alpha = 1.2$) and high volatility ($\sigma = 0.1$). The initial distribution diffuses very quickly, making the transition almost imperceptible.

4.6 Set 4 : $\beta = 2$, $c_0 = 0.01$, $c_1 = 2$, $\alpha = 1.5$, $\sigma = 0.2$

4.6.1 Contours of U (HJB)

The contours of U show a very different structure, with very weak gradients and very broad diffusion. This may be due to extremely strong congestion ($\alpha = 1.5$) and very high volatility ($\sigma = 0.2$). Decisions made early in the period have very diffuse impact, resulting in very smooth variation of U with x.

4.6.2 Contours of M (Fokker-Planck)

The contours of M show very weak diffusion, with a very sharp transition between the two nodes. This may be due to extremely strong congestion ($\alpha = 1.5$) and very high volatility ($\sigma = 0.2$). The initial distribution remains very concentrated, making the transition very marked.

4.7 Set 5 : $\beta = 2$, $c_0 = 1$, $c_1 = 3$, $\alpha = 2$, $\sigma = 0.002$

4.7.1 Contours of U (HJB)

The contours of U show a very different structure, with very weak gradients and very broad diffusion. This may be due to extremely strong congestion ($\alpha = 2$) and very low volatility ($\sigma = 0.002$). Decisions made early in the period have very diffuse impact, resulting in very smooth variation of U with x.

4.7.2 Contours of M (Fokker-Planck)

The contours of M show very weak diffusion, with a very sharp transition between the two nodes. This may be due to extremely strong congestion ($\alpha = 2$) and very low volatility ($\sigma = 0.002$). The initial distribution remains very concentrated, making the transition very marked.

4.8 U and M as Functions of Time

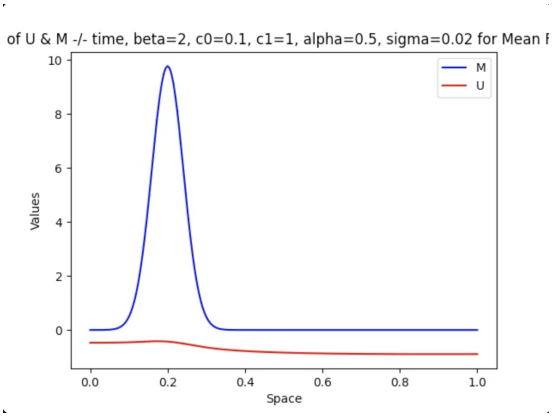

Figure 5: U and M at initial time

For parameter set 1, with weak congestion, the probability density M has a Gaussian shape, and its mean converges toward the minimum of the function U.

Conversely, for parameter set 2 with much stronger congestion, we observe a sort of superposition of two Gaussians, indicating a dual regime.

For parameter set 5, the volatility is much lower than in other cases, the speed of movement toward the minimum is much slower, and two distinct regimes clearly appear.

For parameter set 3, the volatility is high and the movement speed is fast, but the players don't have enough time to make decisions.

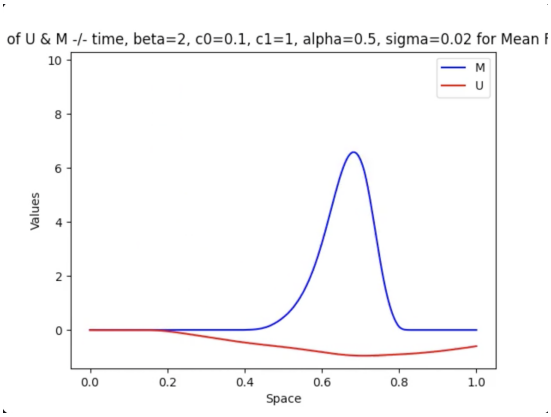

(a) U and M at final time (parameters set 1)

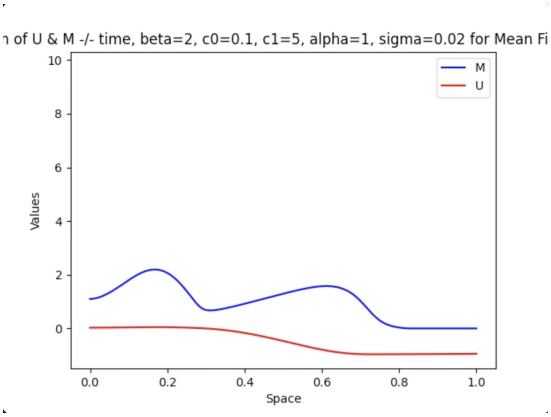

(b) U and M at final time (parameters set 2)

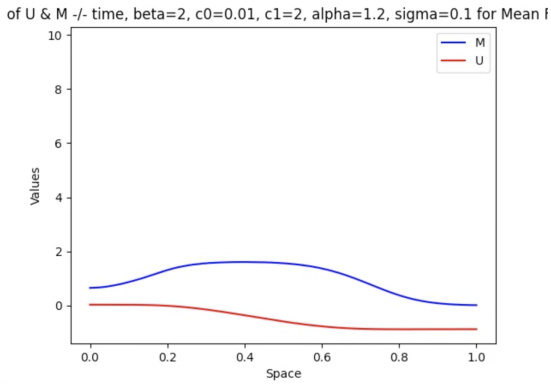

(c) U and M at intermediate time (parameters set 3)

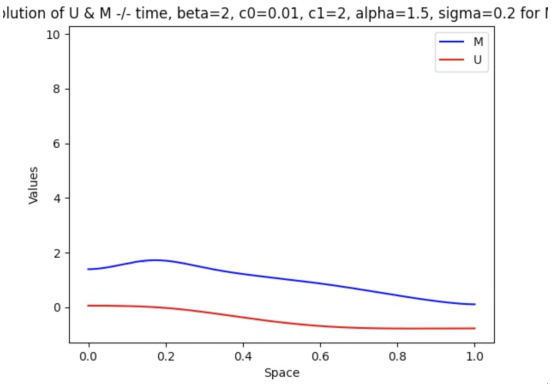

(d) U and M at intermediate time (parameters set 4)

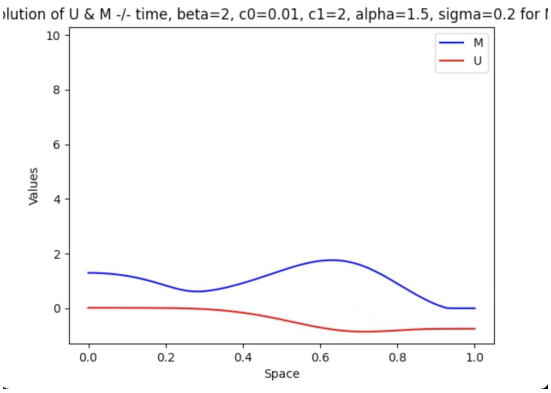

(e) U and M at final time (parameters set 4)

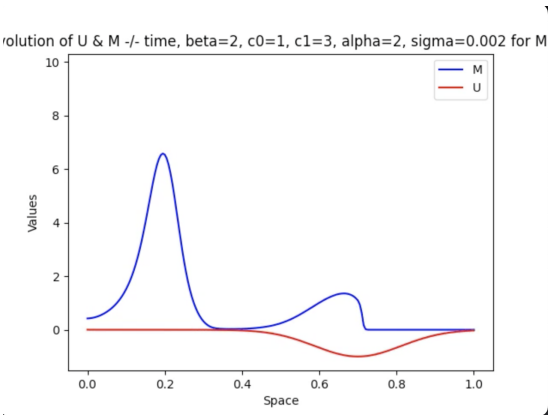

(f) U and M at final time (parameters set 5)

5 Mean Field Control

While MFGs study Nash equilibria in games with infinite selfish players, MFC assumes all agents follow a common strategy optimized for a global objective. This approach is useful, for example, when a planner controls a crowd of agents (like robots) that interact through global or local quantities.

The asymptotic behavior of agents is described by McKean-Vlasov theory, where the dynamics of a representative agent depends on the statistical distribution of states (the mean field). Unlike MFGs where other players' strategies are fixed, in MFC, perturbations of the common strategy directly affect the mean field. This leads to a control problem where the objective is to optimize a global cost function.

MFC gives rise to a forward-backward partial differential equation (PDE) system, similar to MFGs, but which can be interpreted as the optimality conditions of a minimization problem. These problems have applications in finance and risk management, particularly when the state distribution influences the dynamics or cost function.

The system of partial differential equations (PDEs) that arises in mean field control is as follows:

$$\begin{aligned} -\frac{\partial u}{\partial t}(t,x) - \nu\frac{\partial^2 u}{\partial x^2}(t,x) + \frac{1}{\beta}\frac{\left|\frac{\partial u}{\partial x}(t,x)\right|^\beta}{(c_0 + c_1 m(t,x))^\alpha} - \frac{c_1\alpha}{\beta}\frac{m(t,x)\left|\frac{\partial u}{\partial x}(t,x)\right|^\beta}{(c_0 + c_1 m(t,x))^{\alpha+1}} \\ = g(x) + \tilde{f}_0(m(t,x)) + m(t,x)\tilde{f}_0'(m(t,x)), \quad \text{in } [0,T)\times\Omega, \end{aligned} \tag{12}$$

$$\frac{\partial m}{\partial t}(t,x) - \nu\frac{\partial^2 m}{\partial x^2}(t,x) - \frac{\partial}{\partial x}\left(\frac{m(t,\cdot)}{(c_0 + c_1 m(t,\cdot))^\alpha}\left|\frac{\partial u}{\partial x}(t,\cdot)\right|^{\beta-2}\frac{\partial}{\partial x}u(t,\cdot)\right)(x) = 0, \quad \text{in } (0,T]\times\Omega, \tag{13}$$

with Neumann boundary conditions:

$$\frac{\partial u}{\partial x}(t,0) = \frac{\partial u}{\partial x}(t,1) = 0, \quad \text{on } (0,T), \tag{14}$$

$$\frac{\partial m}{\partial x}(t,0) = \frac{\partial m}{\partial x}(t,1) = 0, \quad \text{on } (0,T), \tag{15}$$

and the terminal and initial conditions:

$$u(T,x) = \phi(x), \quad m(0,x) = m_0(x), \quad \text{in } \Omega. \tag{16}$$

It can be shown that if $\beta > 1$, $0 \le \alpha < 1$ and $\tilde{f}_0$ is convex, then there exists a unique solution to this system.

Numerically, we face a very similar situation, though the Jacobian matrix for solving the HJB equation needs to be modified.

5.1 Jacobian Matrix 2

Let $\mathcal{F}_i$ denote the i-th component of $\mathcal{F}(U^n, U^{n+1}, M^{n+1})$.

After calculations, we obtain a tridiagonal Jacobian matrix. We then have:

$$\frac{\partial \mathcal{F}_i}{\partial U^n_{i-1}} = -\frac{\nu}{h^2} - \left(\frac{1}{h^\beta (c_0 + c_1 M_i)^\alpha} + \frac{c_1 \alpha M_i}{h^\beta (c_0 + c_1 M_i)^{\alpha+1}}\right)(U^n_i - U^n_{i-1})_+ \left((U^n_{i+1} - U^n_i)^2 + (U^n_i - U^n_{i-1})^2\right)^{\beta/2-1}$$

$$\frac{\partial \mathcal{F}_i}{\partial U^n_i} = \frac{1}{\Delta t} + \frac{2\nu}{h^2} + \left(\frac{1}{h^\beta (c_0 + c_1 M_i)^\alpha} - \frac{c_1 \alpha M_i}{h^\beta (c_0 + c_1 M_i)^{\alpha+1}}\right)\left((U^n_{i+1} - U^n_i)_- + (U^n_i - U^n_{i-1})_+\right)\left((U^n_{i+1} - U^n_i)^2 + (U^n_i - U^n_{i-1})^2\right)^{\beta/}$$

$$\frac{\partial \mathcal{F}_i}{\partial U^n_{i+1}} = -\frac{\nu}{h^2} - \left(\frac{1}{h^\beta (c_0 + c_1 M_i)^\alpha} + \frac{c_1 \alpha M_i}{h^\beta (c_0 + c_1 M_i)^{\alpha+1}}\right)(U^n_{i+1} - U^n_i)_- \left((U^n_{i+1} - U^n_i)^2 + (U^n_i - U^n_{i-1})^2\right)^{\beta/2-1}$$

6 Comparison with Mean Field Control

We also implemented a numerical scheme for the Mean Field Control (MFC) problem and compared results with MFG. The differences between both approaches are discussed. We plotted U and M curves for both mean field types with identical parameters: $\beta = 2$, $c_0 = 0.1$, $c_1 = 1$, $\alpha = 0.5$ and $\sigma = 0.02$.

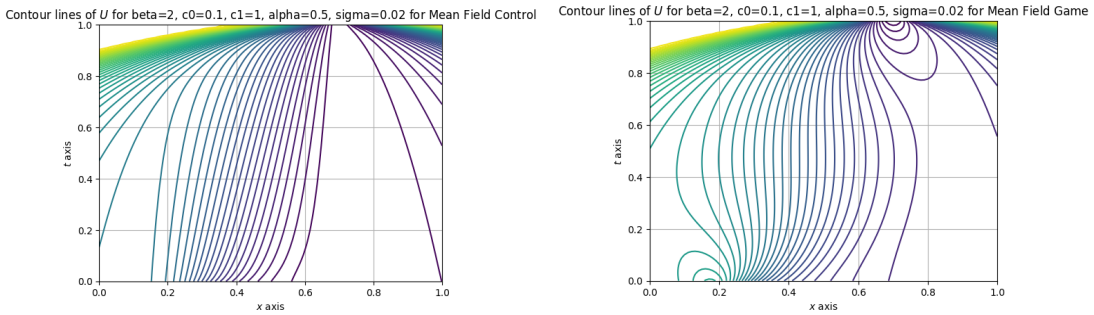

Figure 7: HJB solution for MFC (left) and HJB solution for MFG (right)

We observe that both figures are similar at $t = 1$, which can be explained by identical initialization. However, in the MFG case, we notice looping patterns returning to this state, with more vertical contours compared to MFC which shows no loops and exhibits straighter characteristics as t decreases. This can be interpreted as follows: In MFC, the optimal control is global and acts on all players collectively, preventing these loops and creating a more linear dynamic toward the final solution. Furthermore, in MFG, the contours appear more rounded because each player optimizes their own objective relative to others, leading to more gradual information diffusion and more heterogeneous strategies.

We also plot the density functions M solving the Fokker-Planck equation:

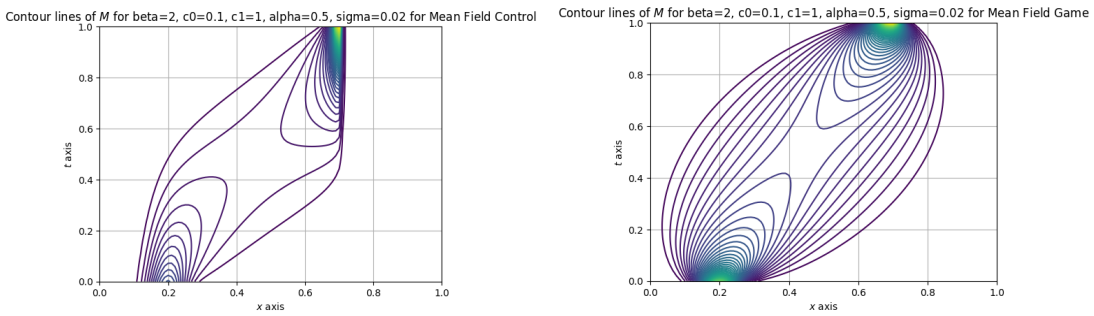

Figure 8: Fokker-Planck solution for MFC (left) and Fokker-Planck solution for MFG (right)

The MFC solution shows strong trajectory centralization: agents are pushed toward a single target in a more constrained manner. In contrast, MFG allows greater flexibility: each agent adapts their behavior based on others, resulting in more natural and less strictly directed trajectories.

7 Conclusion

This project enabled numerical simulation of mean field games with congestion effects. The results align with theoretical predictions and demonstrate the significance of congestion effects in agent dynamics. The comparison with mean field control proved particularly instructive.

Appendix

Questions and Demonstrations

Question 1: Mass Conservation of M^n

The total mass $\sum_{i=0}^{N_h-1} M_i^n$ is conserved due to Neumann boundary conditions. The discrete Fokker-Planck equationreads:

$$(D_t M_i)^n - \nu(\Delta_h M^{n+1})_i - \mathcal{T}_i(U^n, M^{n+1}, \widetilde{M}^{n+1}) = 0.$$

Summing over all spatial indices i, the discrete divergence terms $\mathcal{T}_i$ and diffusion term $\sum_i(\Delta_h M^{n+1})_i$ cancel out through discrete integration by parts, thanks to homogeneous Neumann conditions (19b)-(19c). Thus, the total mass remains constant at each time step:

$$\sum_{i=0}^{N_h-1} M_i^{n+1} = \sum_{i=0}^{N_h-1} M_i^n.$$

Question 2: Uniqueness in the Discrete HJB Equation

Assume two solutions U^n and V^n of the discrete HJB equation (17a)-(17d). Let $W^n = U^n - V^n$. At terminal time $n = N_T$, $W^{N_T} = 0$ according to (17d). By backward induction, assume $W^{n+1} = 0$. The equation (17a) for U^n and V^n yields:

$$-\frac{W^n}{\Delta t} - \nu\Delta_h W^n + \hat{H}([\nabla_h U^n]_i, M_i^{n+1}) - \hat{H}([\nabla_h V^n]_i, M_i^{n+1}) = 0.$$

By monotonicity of the discrete Hamiltonian $\hat{H}$ (property $\hat{\mathbf{H}}_1$), if W^n attains a positive maximum at (n_0, i_0), then $\hat{H}([\nabla_h U^{n_0}]_{i_0}, \cdot) \leq \hat{H}([\nabla_h V^{n_0}]_{i_0}, \cdot)$, which contradicts the equation. Thus, $W^n \leq 0$. Repeating the argument for $-W^n$ shows $W^n \geq 0$. By double inequality, $W^n = 0$, proving uniqueness of the solution.

Question 3: Uniqueness in the Discrete KFP Equation

We know that finding M_{n+1} given M_n and $(U_n)_n$ amounts to solving equation 29:

$$(I_{N_h} - \nu\Delta t D_x^2 + \Delta t(JH)^T)M_{n+1} = M_n$$

Let us denote:

$$B = I_{N_h} - \nu\Delta t D_x^2 + \Delta t(JH)^T$$

We will show that B^T is an M-matrix.

First, for all $0 \leq i < N_h$, we have $B_{i,i}^T = B_{i,i} > 0$. Indeed:

$$B_{i,i} = 1 + \frac{2\nu\Delta t}{h^2} + \Delta t \cdot (JH)_{i,i}^T > 0$$

which is strictly positive by recalling the form of JH in equations (19)-(21).

Second, for $j \neq i$, we have:

$$B_{i,j}^T \leq 0$$

since:

$$B^T_{i,j} = -\frac{\nu \Delta t}{h^2} + \Delta t \cdot (JH)_{i,j} \leq 0$$

Finally, the property $\sum_{j=0}^{N_h-1} B^T_{i,j} > 0$ follows because the row sums of both JH and D_x^2 are zero, yielding:

$$\sum_{j=0}^{N_h-1} B^T_{i,j} = 1 - \nu \Delta t \cdot 0 + \Delta t \cdot 0 = 1 > 0$$

Thus, B^T satisfies the M-matrix property, implying B^T is invertible, and consequently so is B. Therefore, the system $BM_{n+1} = M_n$ admits a unique solution $M_{n+1} \in \mathbb{R}^{N_h}$, proving uniqueness for the discrete KFP equation.

Question 4: Positivity of M^n

From the previous question, we know $(M_n)_n$ satisfies:

$$M_{n+1} = B^{-1} M_n$$

with B^T being an M-matrix. It follows that all entries of $(B^T)^{-1}$ are non-negative, and thus so are those of B^{-1}.

Consequently, whenever $M_n \geq 0$, we must have $M_{n+1} \geq 0$. Starting from $M_0 \geq 0$, we obtain $M_1 \geq 0$, then $M_2 \geq 0$, and so forth. Therefore, $M_0 \geq 0$ implies M_n remains positive for all n.

Codes et Scripts

References

- Y. Achdou et I. Capuzzo-Dolcetta, *Mean field games: numerical methods*, SIAM J. Numer. Anal., 48 (2010), pp. 1136-1162.
- J.-M. Lasry et P.-L. Lions, *Mean field games*, Jpn. J. Math., 2 (2007), pp. 229-260.